Published in final edited form as:
DNA Repair (Amst). 2010 July 1; 9(7): 824–834. doi:10.1016/j.dnarep.2010.04.007.

The *Saccharomyces cerevisiae RAD9*, *RAD17* and *RAD24* genes are required for suppression of mutagenic post-replicative repair during chronic DNA damage

Akiko Murakami-Sekimata[†,*], **Dongqing Huang**[*], **Brian D. Piening**, **Chaitanya Bangur**, and **Amanda G. Paulovich**[§]
Fred Hutchinson Cancer Research Center, 1100 Fairview Avenue N., P.O. Box 19024, Seattle, Washington 98109-1024, USA

Abstract

In *Saccharomyces cerevisiae*, a DNA damage checkpoint in the S phase is responsible for delaying DNA replication in response to genotoxic stress. This pathway is partially regulated by the checkpoint proteins Rad9, Rad17 and Rad24. Here, we describe a novel hypermutable phenotype for *rad9*Δ, *rad17*Δ and *rad24*Δ cells in response to a chronic 0.01% dose of the DNA alkylating agent MMS. We report that this hypermutability results from DNA damage introduction during the S phase and is dependent on a functional translesion synthesis pathway. In addition, we performed a genetic screen for interactions with *rad9*Δ that confer sensitivity to 0.01% MMS. We report and quantify 25 genetic interactions with *rad9*Δ, many of which involve the post-replication repair machinery. From these data, we conclude that defects in S phase checkpoint regulation lead to increased reliance on mutagenic translesion synthesis, and we describe a novel role for members of the S-phase DNA damage checkpoint in suppressing mutagenic post-replicative repair in response to sublethal MMS treatment.

1. Introduction

The DNA damage response (DDR) consists of a highly coordinated network of cellular processes tasked with maintaining genomic integrity despite continual damage from a wide variety of endogenous and exogenous agents. A critical step in this response is cell cycle arrest, in which a damage-induced signal triggers a checkpoint at G1, intra-S, or G2/M[1–3]. Notably, mutations in genes involved in DDR checkpoints are associated with predisposition to cancer in mammals (e.g. ATM, BRCA1, p53) [4].

Methylmethanesulfonate (MMS) is a monofunctional alkylating agent which generates methylated DNA lesions and triggers checkpoint activation; it is commonly referred to as “radiomimetic”[5]. Multiple pathways coordinate to repair MMS lesions, which include direct

[§]Corresponding author: Amanda G. Paulovich, Fred Hutchinson Cancer Research Center, 1100 Fairview Avenue N., LE-360, P.O. Box 19024, Seattle, Washington 98109-1024, Tel: 206-667-1912, Fax: 206-667-2277, apaulovi@fhcrc.org.
[†]Present address: Department of Health Sciences, Graduate School of Medicine, Tohoku University, 2-1 Seiryo, Aoba-ku, Sendai 980-8575, Japan
[*]These authors contributed equally to this work.

Conflict of interest
The authors declare that there are no conflicts of interest.

reversal (dependent on the *MGT1* alkyltransferase), base and nucleotide excision repair, post-replication repair, and homologous recombinational repair[6]. In response to sublethal doses of DNA alkylating agents, budding yeast synchronize into a lengthened S-phase due to an intra-S phase checkpoint that is dependent on *RAD53* and *MEC1*[3]. While the budding yeast checkpoint adapter Rad9 is required for DNA damage-induced arrest in the G1 and G2/M phases, its role in intra-S is not absolute, since deletion of *RAD9* is associated with partial loss of S phase slowing in response to MMS[7]. Members of the *RAD24* epistasis group (RAD24, RAD17, DDC1 and MEC3) exhibit a similar partial defect in S phase slowing[7–9]; however members of this group can enhance the MMS sensitivity of *rad9*Δ[7].

RAD9 has homology to the mammalian BRCA1 gene. Like BRCA1, Rad9 has BRCT and Tudor domains, which are important for protein-protein interactions mostly involved in DNA repair or cell cycle regulation[10]. Rad9 serves as an adapter in the Mec1/Tel1-dependent checkpoint response to DNA damage. An early step in the cellular response to DNA damage is modification of histone tails near the site of damage (e.g. methylation, *MEC1*- or *TEL1*-dependent phosphorylation). Rad9p is subsequently recruited to the damaged site (through the association of its Tudor domains with phosphorylated histone H2A and methylated histone H3) and oligomerizes via its BRCT domains[11]. Once recruited to the damaged site, Rad9p is also phosphorylated in a Mec1/Tel1-dependent manner, and its phosphorylated S/T-Q residues create a binding site for the FHA domain of the checkpoint effecter kinase Rad53 [12–17]. Thus, oligomeric assembly of phosphorylated Rad9p is likely to serve as a platform for the enrichment of Rad53p and stimulation of its trans-autophosphorylation and phosphorylation by Mec1p and Tel1p. These phosphorylation events activate Rad53p and allow it to trigger downstream events in the DDR[18,19].

Members of the *RAD24* epistasis group comprise a damage-specific DNA clamp known as the 9-1-1 complex, which is involved in DNA damage checkpoint regulation. The 9-1-1 clamp is composed of three subunits, Rad17, Ddc1 and Mec3. It is loaded on to the damage site by the alternative heteropentameric replication factor C (RFC) complex, in which one subunit, Rfc1, is replaced by the checkpoint-specific subunit Rad24[20]. Mec1-dependent phoshorylation and activation of Rad9 and Rad53 is severely reduced in *rad17*, *mec3*, *ddc1* and *rad24* mutants [21]. Putative functions of the 9-1-1 complex involve activation of Mec1 kinase activity and recruitment of other factors that could propagate the checkpoint response pathway or facilitate the processivity of the replication fork[21,22].

Both *RAD9* and the *RAD24* group encode for proteins that are required for efficient S-phase checkpoint regulation in response to alkylation damage, and the role of this checkpoint is believed to be to allow a damaged cell time to repair DNA lesions prior to the arrival of the replication fork[23]. If lesions are left unrepaired, cells utilize one of three independent post-replication repair (PRR) mechanisms to bypass the lesion[24]. In the first PRR mechanism, a switch to an error-prone translesion synthesis (TLS) polymerase occurs, which is triggered by a Rad6-Rad18 mediated mono-ubiquitination of PCNA. One of the TLS polymerases is the Polζ complex, composed of Rev3, Rev7, Rev1, and likely additional proteins. Polζ is able to replicate over a damaged template much more efficiently than major replicases, inserting a noncognate nucleotide[25]. A second mechanism employs polyubiquitination of PCNA by the Mms2-Ubc13-Rad5 complex, which promotes error-free lesion bypass through a mechanism involving regression of the replication fork[26]. A third mechanism depends on Rad52, which promotes homologous recombination (HR) between sister chromatids[27]. Genetic interactions between *RAD9* and PRR genes (e.g. *MMS2*, *REV3*) have been reported[28].

In this study, we describe a novel hypermutable phenotype for mutants lacking *RAD9* or members of the *RAD24* epistasis group. We show that the phenotype occurs exclusively when cells are treated with a chronic low-dose treatment of MMS, and not when a higher dose is

applied. Importantly, we demonstrate that different doses of MMS yield different effects on the cell cycle distribution, a phenomenon which is responsible for the dose-dependent hypermutability of S-phase checkpoint mutants. We show that the hypermutable phenotype of *rad9*Δ cells is dependent on *rev3*Δ, indicating that the mutability of such cells is due to hyperactivation of the error-prone post-replication repair pathway. Consistent with (and extending) previous work linking *RAD9* to the PRR pathway, we show that *RAD9* interacts with a large number of PRR genes that function in both error-prone (*REV1*, *REV3*, *REV7*) and error-free (*RAD5*, *MMS2*, *UBC13*) pathways, and present a model in which *RAD9* plays a role in channeling lesions at the replication fork.

2. Materials and Methods

2.1 Media and growth conditions

YEPD and dropout media have been previously described[29]. MMS was purchased from Sigma (Cat# M4016). YEPD and synthetic plates containing MMS were freshly prepared the evening prior to use. Magic medium (SC-Leu-His-Arg; 200mg/L G418, 60mg/L L-Canavanine) used in the synthetic interaction screen was prepared according to Pan *et al*.[30]

2.2 Yeast strains

S. cerevisiae strains used in this study are listed in Table 1. Strain BY4741 was purchased from Open Biosystems. Yeast strains with the designation yMP have been previously described[7]. All gene disruptions were achieved by homologous recombination at their chromosomal loci by standard PCR-based methods[31]. Briefly, a deletion cassette with a 0.5 kb region flanking the target ORF was amplified by PCR from the corresponding *xxx*Δ*KAN*^{r} strain of the deletion array (Open Biosystems) and transformed into the target strain for gene knockout. The primers used in the gene disruptions are designed using 20 bp sequences which are 0.5 kb upstream and downstream of the target gene.

2.3 *rad9*Δ double-deletion library construction and screening

The *rad9*Δ double deletion library was constructed using the dSLAM methodology[32]. The pooled heterozygous diploid deletion library was a gift from Jef Boeke (Johns Hopkins). A *rad9*Δ deletion cassette with a 1.5 kb region flanking the *RAD9* ORF was amplified by PCR (forward primer: 5′-AGCTCTTGAACAACATACTCTCAG-3′; reverse primer: 5′-GAGATTCATCAAACAGATTGATCGC-3′) and transformed into the library. Selection of the *rad9*Δ::*URA3* diploids was performed on synthetic defined medium plates without uracil (SD-URA). Diploids were subsequently sporulated via replication onto SPO plates and incubation at room temperature for 5 days. Spores were replicated onto Magic Medium (MM) –URA plates to select *MAT***a** *rad9*Δ::*URA3* double mutant haploid cells. Haploid double-deletion cells were replicated onto complete synthetic medium with or without 0.01% MMS. Clones exhibiting sensitivity to MMS were streaked for single colonies on complete SD-medium. Eight colonies per candidate were subsequently grown overnight in synthetic liquid medium to saturation, and 2μl of saturated culture were spotted on complete SD-medium +/− 0.01% MMS and scored after 2–3 days. For each candidate, UPTAG and DOWNTAG barcodes were sequenced to identify the corresponding gene deletion using primers and methods previously described[33,34].

2.4 MMS kill curves and cell cycle analysis

MMS kill curves were performed as previously described[3,7]. Briefly, log-phase cells (5×10^7 cells) were harvested from YPD medium and resuspended in 10 ml YPD with a specified concentration of pre-diluted liquid MMS solution. One MMS solution was used for all cultures in a single experiment to ensure identical MMS concentration across all cultures, and control

strains (wildtype, *xxx*Δ, *and rad9*Δ) were always run on the same day as the double mutants to control for day-to-day variation in MMS preparations. Cultures were incubated at 30°C, and aliquots were taken out at given intervals. The cells were resuspended in PBS + 5% sodium thiosulfate (to inactivate the MMS). Cells were sonicated, and cell concentrations were assessed using a Coulter Counter. Viability was determined by plating serial dilutions of cultures onto YPD and scoring the number of colony-forming units (CFU) after 3–4 days at 30°C. Viability was calculated as CFU/total cells. Cell cycle distributions were determined by flow cytometry of propidium iodide (PI)-stained cells using a method described previously [7]. Distributions of PI-stained cells were assessed using a Beckman Dickson Calibur flow cytometer.

2.5 Ionizing radiation (IR) kill curves

Log-phase cells grown at 30°C in YEPD were harvested, sonicated, and counted using a Coulter Counter. 1×10^8 cells were resuspended in 2 ml PBS, sonicated, and serially diluted. Dilutions were spread onto fresh YEPD plates and exposed to gamma irradiation using a Mark II cesium-137 irradiator (JL Shepherd & Associates) operated at a dose rate of 800 cGy/minute. Following IR, plates were immediately transferred to an incubator, and allowed to grow for 3 days at 30°C. Viability was calculated as CFU/total cells. Control cells were always irradiated on the same day as mutant strains, and three independent isolates were tested for each mutant strain over a three day period.

2.6 MMS-induced mutation and SCE rate

MMS-induced mutation and sister chromatid exchange (SCE) rates were measured as previously described[35]. Briefly, mutation rates were measured by selection for Canavanine resistance (due to forward mutation of the *CAN1* gene). Mutation rates were determined in both the BY4741 and A364a backgrounds. SCE rates were measured in the A364a background, previously engineered to carry a *SCR::URA3* sister chromatid recombination substrate [36, 37]. SCE and mutation rates were measured simultaneously (i.e. side by side on the same days with the same cell cultures) for these studies, and controls were always examined concurrently on the same day alongside mutant strains. MMS treatment of cells was performed exactly the same as described in section 2.4. Following inactivation of the MMS by resuspension of cells in PBS + 5% sodium thiolsulfate, cells were serially diluted and plated onto SD-Arg-Ser + 60 mg/L canavanine medium (for measurement of mutation rates), SD-His medium (for measurement of SCE rates), and YPD medium (for viability). Plates were incubated at 30°C for 3 days, and numbers of mutants/recombinants were assessed by the number of CFUs on the respective selection plates. Mutation rates were expressed as canavanine-resistant cells per 10^6 viable cells. SCE rates were expressed as His^+ cells per 10^6 viable cells. For both mutation and SCE, the rates after MMS induction were determined by subtracting the observed numbers of mutants or recombinants in the starting culture (i.e. pre-MMS exposure) from the number observed post-MMS exposure.

3. Results

3.1 A synthetic sensitivity screen reveals 25 interactions with *RAD9,* many of which involve post-replication repair

Synthetic enhancement genetics can be used to examine how mutations in two genes interact to modulate a phenotype and to uncover useful information about the functions of the interacting genes and their relationship[38]. We performed a genetic screen to identify second site mutations that enhance the DNA damage sensitivity of the *rad9*Δ mutant to chronic sublethal (0.01%) MMS treatment. We utilized a screening protocol derived from the dSLAM procedure[32]. Briefly, a *rad9*Δ*::URA3* query construct was introduced to a haploid-convertible heterozygous diploid yeast knockout library pool by integrative transformation.

Following sporulation, the haploid double mutants carrying both the *rad9*Δ allele and a second gene disruption were selected and subsequently screened for sensitivity on synthetic complete media plates containing 0.01% MMS. A total of 27,000 colonies were screened from the double deletion library. From this, 337 individual double deletion mutants were found to be sensitive to MMS, of which 202 unique double mutants were identified by sequencing of the flanking barcode regions.

Our initial screen was not exclusive for the enhancement phenotype we sought, since all *single* mutants conferring significant sensitivity to MMS also would be recovered (in addition to the desired *rad9*Δ–interacting genes). Thus we performed a quantitative counter screen comparing the sensitivity of each double mutant candidate (*xxx*Δ *rad9*Δ) to the original single mutants (*xxx*Δ) from the deletion library by assessing viability following a 5-hour exposure to 0.01% MMS in liquid rich medium. This counter screen identified a subset of 25 yeast gene disruptions that significantly enhance the sensitivity of the *rad9*Δ mutant, such that the *xxx*Δ *rad9*Δ double mutant was more sensitive to MMS than either the *rad9*Δ or the *xxx*Δ single mutants.

To reconfirm the enhanced sensitivity, we reconstructed individual gene deletions of the 25 genes in a wild type or *rad*9Δ background by mating each single deletion strain to a *rad*9Δ strain. Three independent segregants of each double or single mutant were subjected to a second round of MMS liquid kill curve testing. All 25 of the double mutants (*xxx*Δ *rad9*Δ) exhibited a 5-fold or greater enhanced sensitivity to MMS than either single mutant (*xxx*Δ or *rad9*Δ) ($p<0.01$) (Table 2 and Supplemental Figure S1). These genes comprised a number of different functional categories (Figure 1), and 15 out of the 25 interactions were previously unobserved (indicated by an asterisk in Figure 1). The severity of the interaction with *rad9*Δ varied significantly among these categories (Table 2). Notably, genes involved in PRR exhibited the highest degree of interaction with *rad9*Δ (Table 2 and Supplemental Figure S1). Genes involved in homologous recombination repair (HR) and resolution of HR intermediates as well as direct reversal of alkylation (*MGT1*) and other aspects of DNA repair (*IXR1*) also enhanced the sensitivity of *rad9*Δ.

Interestingly, we also identified a number of genes not previously known to function in the DDR, including *ISW1* (chromatin remodeling), *POT1* (fatty acid metabolism), *BBC1* (localized to actin patches), *MSN1* (transcription), and two uncharacterized genes, *YIL158W* and *UIP5*. In order to determine whether these interactions displayed general DNA damage sensitivity or MMS-specific sensitivity, we tested whether these genes enhanced *rad9*Δ sensitivity to ionizing radiation as well. Four of the candidates (*BBC1*, *ISW1*, *YIL158W* and *POT1*) displayed cross-sensitivity to ionizing radiation, suggesting that these genes are important for surviving DNA damage in *rad9*Δ cells (Supplemental Figure S2).

3.2 The *rad9*Δ mutant shows a dose-dependent, *REV3*-dependent hypermutable phenotype in MMS

Cells have multiple repair options available for handling any single lesion; however the cellular mechanism for choosing which pathway to utilize is poorly understood. In light of results from our screen and recent data linking checkpoint genes to choice of PRR mechanism[39], we sought to explore the role of the *S. cerevisiae* checkpoint gene *RAD9* in such a function. We hypothesized that if *RAD9* contributed to regulation of mutagenic versus error-free PRR in the S phase, then the *rad9*Δ mutant might exhibit a hypermutable phenotype when treated with the DNA alkylating agent MMS. To test this prediction, we exposed cells to 0.01% MMS in liquid culture for 5 hours and assayed induction of mutations by measuring forward mutation to canavanine resistance. As shown in Figure 2A, the *rad9*Δ mutant shows significant elevation of MMS-induced mutation rate compared to wild type ($p\leq0.01$).

At first glance, this result contradicts a previous report by Barbour *et al.* that the *rad9*Δ mutant is *not* hyper-mutable in the presence of MMS[28]. However, we subsequently noted that the MMS exposures were very different between these two studies; in our study, cells were exposed for 5 hours to 0.01% MMS, whereas in the Barbour *et al.* study, cells were exposed to a higher concentration of MMS (0.05%) for half an hour. We hypothesized that this critical difference in exposure might explain the discordant results in the two studies. To test this, we measured MMS-induced mutation rates in the same strains under the two conditions (5 hours at 0.01% MMS vs 0.5 hours at 0.05% MMS; see Figure 2A). Consistent with the report of Barbour *et al.*, we saw no hypermutable phenotype of *rad9*Δ at the 0.05% MMS dose, demonstrating the dose-dependence of the *rad9*Δ hypermutable phenotype (Figure 2A).

To test whether the *rad9*Δ MMS dose-dependent hypermutable phenotype was specific to the BY4741 strain background, we repeated the mutagenesis studies in the A364a strain background. As shown in Figure 2B, the MMS dose-dependent hypermutable phenotype is recapitulated in the A364a background; furthermore, the hypermutable phenotype could also be detected at a ten-fold lower MMS exposure (0.001%) (Figure 2C). We conclude that the hypermutable phenotype of *rad9*Δ in MMS is dose-dependent and is not unique to the BY4741 strain background.

To determine whether the hypermutable phenotype was dependent on the canonical *REV3*-dependent error-prone PRR pathway, we tested whether the recovery of *can1* mutants in the *rad9*Δ background was *REV3*-dependent. We constructed a *rad9*Δ *rev3*Δ double mutant and repeated the mutagenesis experiment. As shown in Figure 2C, the hypermutable phenotype of *rad9*Δ cells is dependent on *REV3*, demonstrating that the hypermutable phenotype is due to increased activity of the error-prone *REV3*-dependent branch of the PRR pathway.

In addition to mutagenic damage tolerance mechanisms, PRR can also employ homologous recombination (HR), which can be tested by measuring sister chromatid exchange (SCE) rates. Thus, we asked whether *rad9*Δ has an effect on SCE induction in the presence of MMS. We observed that wild type and *rad9*Δ cells exhibited no significant difference in SCE induction in either the 0.01% (5 hours) or the 0.05% (0.5 hours) MMS conditions (Figure 2B). Thus, we conclude that while *rad9*Δ mutation affects MMS-inducible mutation rates, there is no effect on the rate of MMS-inducible SCE in these cells.

3.3 The dose-dependence of the hypermutable phenotype in *rad9*Δ correlates with differences in cell cycle distribution in response to different doses of MMS

One possible explanation for the dose-dependence of the *rad9*Δ hypermutable phenotype is that in 0.05% MMS, lesion density is high enough to produce multiple lesions in a short track of DNA, which is more likely to degrade or be processed to a DSB than to induce mutagenic trans-lesion synthesis. However, our data do not support this model. For example, if more DSB were being produced in the 0.05% versus 0.01% MMS conditions, we would expect to see higher rates of sister chromatid recombination in the former. In contrast, we see a higher level of sister chromatid exchange induction in the 0.01% MMS conditions (Figure 2B). Also *not* consistent with there being more DSB in the 0.05% conditions, the 0.01% MMS condition introduces more lethal damage (DSBs are lethal in haploid yeast cells), evidenced by lower survival of *rad9*Δ, indicating that a concentration of 0.01% MMS at 5 hrs is a higher *effective dose* than 0.05% MMS at ½ hour. Thus it is unlikely that the possibility of fewer DSBs at the lower concentration explains the hypermutable phenotype.

Since it has been documented that DNA repair and DNA damage tolerance mechanisms differ throughout the cell cycle[36,40], a second possible explanation for the dose-dependence of the *rad9*Δ hypermutable phenotype is that cell cycle distributions differ significantly between the 0.01% and 0.05% MMS conditions used in these studies. (We previously demonstrated that

0.015 – 0.03% MMS exposure induces a regulated slowing of S phase progression, termed the intra-S phase checkpoint[3,7,40]; the 0.05% dose used in the Barbour *et al.* study was not previously tested for S phase effects.) To test this hypothesis, we treated wild type and *rad9*Δ cells with either 0.01% or 0.05% MMS for a period of 5 hours, withdrawing cells at multiple time points throughout the treatment for assessment of cell cycle distribution by flow cytometry. As seen in Figure 3A, wild type cells treated with 0.01% of MMS accumulate in the S phase over the course of 5 hours, as previously described[3,7]. Also as previously described[7], *rad9*Δ cells treated with the same dose show reduced accumulation in the S phase, proceeding through to the G2 phase faster than wild type. In dramatic contrast, there is no observable accumulation of *rad9*Δ cells in the S phase during a 30 minute pulse of an asynchronous culture with 0.05% MMS (Figure 3A), the conditions used in the Barbour *et al.* study. Based on these data, the majority of MMS-induced DNA damage in our experiments (0.01% MMS) is introduced during the S phase of the cell cycle, whereas the majority of damage was induced outside of the S phase in the 0.05% MMS condition used in the Barbour et al. study. Moreover, if we treat cells with 0.05% MMS past the 30 minute pulse, we see a synchronization represented by a strong G1 peak (Figure 3A). We confirmed that these cells were accumulating in the G1 phase through the observation that the majority of cells at the higher dose remain unbudded (Figure 3B). However, a proportion of budded cells remain, suggesting that though replication is suppressed, it may not entirely be due to accumulation in the G1 phase. It is possible that a small proportion of cells progress into the S phase upon treatment with 0.05% MMS, but the replication forks may only progress for very small distances in response to high doses (producing a “G1-like” S-phase peak). Nonetheless, these results are consistent with the hypothesis that the defect in the intra-S phase checkpoint in *rad9*Δ cells leads to a higher mutation rate in the 0.01% MMS treatment (where cells are replicating), but not in the 0.05% MMS treatment (where replication is suppressed). Importantly, it has been demonstrated that cells are most susceptible to mutagenesis in the S phase of the cell cycle[40].

If the dose-dependent *rad9*Δ hypermutable phenotype were due to a defect in the intra-S phase DNA damage checkpoint, then we predicted that other mutations (e.g. *rad17*Δ and *rad24*Δ) affecting this checkpoint might also exhibit dose-dependent hypermutability in MMS[7]. To test this prediction, we measured mutation and SCE induction in *rad17*Δ and *rad24*Δ mutants in 0.01% MMS. As shown in Figure 3C, the *rad17*Δ and *rad24*Δ mutants phenocopy *rad9*Δ, displaying hypermutability in response to a 5 hour exposure to 0.01% MMS, but no effect on MMS-induced SCE. Like *rad9*Δ, both *rad17*Δ and *rad24*Δ mutants display reduced accumulation in the S-phase after chronic MMS treatment[7], a phenotype that is not evident following a pulse of 0.05% MMS (Supplemental Figure S3). The observation that additional intra-S phase checkpoint-defective mutants exhibit similarly enhanced MMS-inducible mutation rates is consistent with a model wherein the hypermutable phenotype is a result of inappropriate S-phase progression in the presence of MMS-induced damage.

4. Discussion

4.1 DNA damage, *RAD9* and the S phase

As described in this study, MMS dose has a profound impact on cell cycle distributions. In the previous study by Barbour *et al.*[28], a rapid 30 minute pulse with 0.05% MMS is not associated with accumulation of cells in S phase (Figure 3), and base excision repair is likely to remove alkylation damage, in most cases prior to entry into the S phase (after the MMS is withdrawn). As a result, there is little consequence to the genetic integrity of the cell. However, if residual damage remains once cells enter the S phase, or if damage is introduced during the S phase (as is the case in the 0.01% MMS condition used in our experiments), replication forks encounter the damage and stall, and cells are forced to employ damage tolerance mechanisms, some of

which are mutagenic. This hypothesis is consistent with studies of Ostroff *et al.* and Kadyk *et al.* that demonstrated that cells are most susceptible to UV-induced mutagenesis and sister chromatid exchange during the S phase of the cell cycle[37,40].

There are three potential outcomes for a stalled replication fork (Figure 4). First, DNA repair proteins (e.g. base excision repair) may remove the offending lesion, allowing the fork to resume replication. Second, the lesion can be tolerated (i.e. circumnavigated, rather than being removed) either by template switching (dependent on *MMS2*, *UBC13*, *RAD5*) or by mutagenic translesion synthesis (dependent on *REV1*, *REV3*, *REV7*). Third, the stalled fork may collapse, and occasional fork collapses are repaired by homologous recombination (HR) [41]. *MEC1* is required for stabilizing stalled forks; hence in the *mec1* mutant stalled forks collapse irreversibly at high rates, resulting in rapid death[42].

Our genome-wide screen revealed extensive interactions between *RAD9* and post-replication repair genes required for tolerating unrepaired DNA damage during the S phase. We can infer from the heightened importance of post-replication repair in *rad9Δ* cells that replication forks are encountering lesions more frequently in the *rad9Δ* mutant than in the wild type. This could be due to: i) a general decrease in the efficiency of repair or reversal of alkylation damage in the *rad9Δ* mutant, and/or ii) abnormal coordination between DNA replication and alkylation damage repair or reversal in the *rad9Δ* mutant, resulting in an increase in the number of lesions' being encountered by replication forks. There are data suggesting that either or both of these mechanisms could occur, as discussed below.

RAD9 has been implicated in nucleotide excision repair of UV-damaged DNA[43,44]. Recent studies have suggested that *RAD9* is required for repair of the transcribed strands and the non-transcribed strands of active genes (but not for repair of transcriptionally inactive DNA sequences), possibly through the up-regulation of genes involved in the repair process[45]. There are no studies reported to look for a role, either direct or indirect, of *RAD9* in promoting base excision repair or direct reversal of alkylation damage, and this would be an interesting area of follow-up investigation.

We previously showed that in the continuous presence of MMS, the rate of S phase progression is dramatically slowed by an intra-S phase checkpoint in wild type cells[3], suggesting the possibility that there may be coordination between DNA replication and repair. It is interesting to note that while *mec1* and *rad53* mutants show severe defects in S phase regulation in the presence of MMS, *rad9*Δ mutation confers a far more subtle defect [7]. The basis of these two distinct phenotypes is not understood, and it is equally plausible that *MEC1* (or *RAD53*) and *RAD9* are involved in distinct mechanisms controlling S phase progression or that they are involved in the same mechanism, with the *MEC1* and *RAD53* mutations showing higher penetrance. Of note, the *mec1 rad9*Δ and *rad53Δ rad9*Δ double mutants are more sensitive to MMS then any of the single mutants [7], indicating that the survival-promoting functions of *MEC1* and *RAD53* do not lie completely within the same pathway as that for *RAD9*.

Elegant work by Tercero and Diffley[42] investigated the underlying mechanism of S phase slowing in the presence of MMS, and the effects of mutations in *RAD53* and *MEC1*. They showed that exposure to MMS reduces the rate of DNA replication fork progression to about 300 base pairs per minute, 5 to 10 times lower than fork rates in the absence of MMS[46,47]. However, they found that the slow fork rate progression does not require *RAD53* or *MEC1*, indicating that the accelerated S phase is primarily a consequence of inappropriate initiation events observed in these mutants. Furthermore, the cytotoxicity of MMS in checkpoint mutants occurs specifically when cells are allowed to enter S phase with damage, at which time replication forks in checkpoint mutants collapse irreversibly at high rates. Hence, preventing damage-induced replication fork catastrophe seems to be a primary mechanism by which the

MEC1-dependent checkpoint preserves viability in the face of DNA alkylation. (Of note, these studies were all performed in the presence of 0.033% MMS.)

The mechanism underlying the *RAD9*-dependent slowing of S phase progression in response to MMS has not been investigated, nor have fork elongation rates been measured in the *rad9Δ* mutant in the presence of low dose MMS (i.e. 0.01% MMS during active S phase). Hence, while the Tercero and Diffley [42] data eliminate the possibility of *MEC1*-dependent control of replication fork elongation (at least in 0.033% MMS), their data do not eliminate the possibility that fork elongation rate is controlled in a *MEC1*-independent mechanism. Hence, although speculative, it remains formally possible that slowing of S phase in response to MMS is due both to control of origin firing (*MEC1*-dependent) and control of elongation, and we hypothesize that control of elongation may be *RAD9*-dependent and required for efficient removal of alkylation damage, via a mechanism potentially analogous to transcription-repair coupling[48].

4.2 Model for *RAD9*'s facilitating the repair or tolerance of DNA damage by regulating the replication fork

Barbour *et al.* proposed that because *rad9*Δ is synergistic to both *mms2* and *rev3* with respect to killing by MMS, *RAD9* likely functions as a separate branch of post-replication repair, independent of the *REV3*- and *MMS2*-associated branches and downstream of *RAD18*. Our observation that *rad9*Δ cells are hypermutable in 0.01% MMS is consistent with this model, in that loss of a parallel post-replication repair pathway could shuttle a higher percentage of DNA lesions into the mutagenic, *REV3*-dependent translesion synthesis pathway. There are alternative models.

One alternative model is that the *RAD9* adapter acts at the replication fork at sites of damage to regulate how DNA damage is channeled through the various repair and tolerance pathways during the S phase so as to minimize genetic instability (Figure 4). Ill-described biochemical acrobatics must occur at the fork to elicit polymerase switching or template switching when DNA damage tolerance mechanisms are employed, and the mechanism of these switches is unclear[49]. Under this alternative model, in the presence of MMS, *RAD9* activity would strongly and *actively promote* use of non-mutagenic base excision repair (and/or alkylation reversal), while it would *actively suppress* mutagenic translesion synthesis. Hence, loss of *RAD9* function would reduce the efficacy of base excision repair (Figure 4), thereby increasing the reliance of cells on template switching and translesion synthesis for survival; this would explain the synergy observed between the *rad9*Δ and both the *mms2*Δ and *rev3*Δ mutants, without evoking the need of a novel post-replication repair pathway. Additionally, loss of *RAD9* function would result in derepression of translesion synthesis (Figure 4), leading to the hypermutable phenotype observed in our experiments. Hence, under this alternative model, *RAD9* does not participate in a third branch of DNA damage tolerance, but rather it stabilizes the genome by maximizing the cell's ability to employ non-mutagenic mechanisms (base excision repair and template switching) of repairing or tolerating lesions, while suppressing mutagenic translesion synthesis.

A second alternative model is that *RAD9* acts to promote continuous DNA synthesis, potentially by limiting re-priming of stalled forks at MMS lesions. In this model, the observed hypermutability in MMS-treated *rad9*Δ cells may be due to an increased reliance on PRR to repair large ssDNA gaps resulting from discontinuous synthesis, which would explain the synergy between *rad9*Δ and both the *MMS2* and *REV3* branches of PRR.

Interactions between *rad9*Δ and HR repair genes are consistent with both models. In the first model, loss of *RAD9* function would result in a higher frequency of fork stalling at unrepaired lesions, leading to an elevated probability of fork collapse and repair by HR genes[41,50]. In

the second model, a number of these HR genes (*SGS1*, *MUS81*, *MMS4* and members of the *RAD52* group) have been shown to promote gap repair and are epistatic to genes in the error-free branch of PRR[51,52,56]. Their synergy with *rad9*Δ may indicate an inability to repair large ssDNA gaps in *rad9*Δ cells. Recent work has shown that the choice among homologous recombination, translesion synthesis, and Rad52-related gap repair is dependent on a complex interplay between ubiquitination and sumoylation of PCNA[53]. The role, if any, that *RAD9* might play in mediating these signaling events is an intriguing avenue for further study.

4.3 Implications for human disease

BRCA1, one putative mammalian homolog of *RAD9*, also plays an important role in S-phase checkpoint regulation and genome stability [54]. It is tempting to speculate that BRCA1 may also have synergistic interactions with homologs of PRR genes characterized in this study. If such synergistic interactions are evident in human cells, such genes may be modifiers of cancer penetrance for *BRCA1* cases. Moreover, inhibition of PRR pathways may serve as an effective treatment mechanism for BRCA1 −/− tumors, comparable to the growing use of poly(ADP-ribose) polymerase (PARP) inhibitors, now in clinical trials for treating BRCA-deficient tumors [55].

Supplementary Material

Refer to Web version on PubMed Central for supplementary material.

Acknowledgments

We thank Jef Boeke for the diploid deletion library pool and Sean Wang for help with statistical analyses. We thank our anonymous reviewers for their insightful comments and suggestions. B.D.P. was supported by the FHCRC Dual Mentor Program and a U.S. Department of Defense Breast Cancer Research Program predoctoral fellowship. This work was supported by NIH grant R01 CA 129604.

References

1. Weinert TA, Hartwell LH. The RAD9 gene controls the cell cycle response to DNA damage in saccharomyces cerevisiae. Science 1988;241:317–322. [PubMed: 3291120]
2. Siede W, Friedberg AS, Friedberg EC. RAD9-dependent G1 arrest defines a second checkpoint for damaged DNA in the cell cycle of saccharomyces cerevisiae. Proc Natl Acad Sci U S A 1993;90:7985–7989. [PubMed: 8367452]
3. Paulovich AG, Hartwell LH. A checkpoint regulates the rate of progression through S phase in S. cerevisiae in response to DNA damage. Cell 1995;82:841–847. [PubMed: 7671311]
4. Walsh T, King MC. Ten genes for inherited breast cancer. Cancer Cell 2007;11:103–105. [PubMed: 17292821]
5. Friedberg, EC.; Friedberg, EC. DNA Repair and Mutagenesis. ASM Press; Washington, D.C: 2006.
6. Xiao W, Chow BL, Rathgeber L. The repair of DNA methylation damage in saccharomyces cerevisiae. Curr Genet 1996;30:461–468. [PubMed: 8939806]
7. Paulovich AG, Margulies RU, Garvik BM, Hartwell LH. RAD9, RAD17, and RAD24 are required for S phase regulation in saccharomyces cerevisiae in response to DNA damage. Genetics 1997;145:45–62. [PubMed: 9017389]
8. Longhese MP, Fraschini R, Plevani P, Lucchini G. Yeast pip3/mec3 mutants fail to delay entry into S phase and to slow DNA replication in response to DNA damage, and they define a functional link between Mec3 and DNA primase. Mol Cell Biol 1996;16:3235–3244. [PubMed: 8668138]
9. Longhese MP, Paciotti V, Fraschini R, Zaccarini R, Plevani P, Lucchini G. The novel DNA damage checkpoint protein ddc1p is phosphorylated periodically during the cell cycle and in response to DNA damage in budding yeast. EMBO J 1997;16:5216–5226. [PubMed: 9311982]
10. Yang XJ. Multisite protein modification and intramolecular signaling. Oncogene 2005;24:1653–1662. [PubMed: 15744326]

11. Conde F, Refolio E, Cordon-Preciado V, Cortes-Ledesma F, Aragon L, Aguilera A, San-Segundo PA. The Dot1 histone methyltransferase and the Rad9 checkpoint adaptor contribute to cohesin-dependent double-strand break repair by sister chromatid recombination in saccharomyces cerevisiae. Genetics 2009;182:437–446. [PubMed: 19332880]
12. Vialard JE, Gilbert CS, Green CM, Lowndes NF. The budding yeast Rad9 checkpoint protein is subjected to Mec1/Tel1-dependent hyperphosphorylation and interacts with Rad53 after DNA damage. EMBO J 1998;17:5679–5688. [PubMed: 9755168]
13. Emili A. MEC1-dependent phosphorylation of Rad9p in response to DNA damage. Mol Cell 1998;2:183–189. [PubMed: 9734355]
14. Soulier J, Lowndes NF. The BRCT domain of the S. cerevisiae checkpoint protein Rad9 mediates a Rad9-Rad9 interaction after DNA damage. Curr Biol 1999;9:551–554. [PubMed: 10339432]
15. Schwartz MF, Duong JK, Sun Z, Morrow JS, Pradhan D, Stern DF. Rad9 phosphorylation sites couple Rad53 to the saccharomyces cerevisiae DNA damage checkpoint. Mol Cell 2002;9:1055–1065. [PubMed: 12049741]
16. Carr AM. DNA structure dependent checkpoints as regulators of DNA repair. DNA Repair (Amst) 2002;1:983–994. [PubMed: 12531008]
17. Usui T, Foster SS, Petrini JH. Maintenance of the DNA-damage checkpoint requires DNA-damage-induced mediator protein oligomerization. Mol Cell 2009;33:147–159. [PubMed: 19187758]
18. Gilbert CS, Green CM, Lowndes NF. Budding yeast Rad9 is an ATP-dependent Rad53 activating machine. Mol Cell 2001;8:129–136. [PubMed: 11511366]
19. Sweeney FD, Yang F, Chi A, Shabanowitz J, Hunt DF, Durocher D. Saccharomyces cerevisiae Rad9 acts as a Mec1 adaptor to allow Rad53 activation. Curr Biol 2005;15:1364–1375. [PubMed: 16085488]
20. Majka J, Burgers PM. Yeast Rad17/Mec3/Ddc1: A sliding clamp for the DNA damage checkpoint. Proc Natl Acad Sci U S A 2003;100:2249–2254. [PubMed: 12604797]
21. Bonilla CY, Melo JA, Toczyski DP. Colocalization of sensors is sufficient to activate the DNA damage checkpoint in the absence of damage. Mol Cell 2008;30:267–276. [PubMed: 18471973]
22. Sabbioneda S, Minesinger BK, Giannattasio M, Plevani P, Muzi-Falconi M, Jinks-Robertson S. The 9-1-1 checkpoint clamp physically interacts with polzeta and is partially required for spontaneous polzeta-dependent mutagenesis in saccharomyces cerevisiae. J Biol Chem 2005;280:38657–38665. [PubMed: 16169844]
23. Paulovich AG, Toczyski DP, Hartwell LH. When checkpoints fail. Cell 1997;88:315–321. [PubMed: 9039258]
24. Andersen PL, Xu F, Xiao W. Eukaryotic DNA damage tolerance and translesion synthesis through covalent modifications of PCNA. Cell Res 2008;18:162–173. [PubMed: 18157158]
25. Nelson JR, Lawrence CW, Hinkle DC. Thymine-thymine dimer bypass by yeast DNA polymerase zeta. Science 1996;272:1646–1649. [PubMed: 8658138]
26. Blastyak A, Pinter L, Unk I, Prakash L, Prakash S, Haracska L. Yeast Rad5 protein required for postreplication repair has a DNA helicase activity specific for replication fork regression. Mol Cell 2007;28:167–175. [PubMed: 17936713]
27. Resnick MA. The repair of double-strand breaks in chromosomal DNA of yeast. Basic Life Sci 1975;5B:549–556. [PubMed: 1103871]
28. Barbour L, Ball LG, Zhang K, Xiao W. DNA damage checkpoints are involved in postreplication repair. Genetics 2006;174:1789–1800. [PubMed: 17057245]
29. Amberg, DC.; Burke, DJ.; Strathern, JN. Methods in Yeast Genetics: A Cold Spring Harbor Laboratory Course Manual. Cold Spring Harbor Laboratory Press; NY: 2005.
30. Pan X, Yuan DS, Ooi SL, Wang X, Sookhai-Mahadeo S, Meluh P, Boeke JD. dSLAM analysis of genome-wide genetic interactions in saccharomyces cerevisiae. Methods 2007;41:206–221. [PubMed: 17189863]
31. Brachmann CB, Davies A, Cost GJ, Caputo E, Li J, Hieter P, Boeke JD. Designer deletion strains derived from saccharomyces cerevisiae S288C: A useful set of strains and plasmids for PCR-mediated gene disruption and other applications. Yeast 1998;14:115–132. [PubMed: 9483801]

32. Pan X, Yuan DS, Xiang D, Wang X, Sookhai-Mahadeo S, Bader JS, Hieter P, Spencer F, Boeke JD. A robust toolkit for functional profiling of the yeast genome. Mol Cell 2004;16:487–496. [PubMed: 15525520]
33. Winzeler EA, Shoemaker DD, Astromoff A, Liang H, Anderson K, Andre B, Bangham R, Benito R, Boeke JD, Bussey H, Chu AM, Connelly C, Davis K, Dietrich F, Dow SW, El Bakkoury M, Foury F, Friend SH, Gentalen E, Giaever G, Hegemann JH, Jones T, Laub M, Liao H, Liebundguth N, Lockhart DJ, Lucau-Danila A, Lussier M, M'Rabet N, Menard P, Mittmann M, Pai C, Rebischung C, Revuelta JL, Riles L, Roberts CJ, Ross-MacDonald P, Scherens B, Snyder M, Sookhai-Mahadeo S, Storms RK, Veronneau S, Voet M, Volckaert G, Ward TR, Wysocki R, Yen GS, Yu K, Zimmermann K, Philippsen P, Johnston M, Davis RW. Functional characterization of the S. cerevisiae genome by gene deletion and parallel analysis. Science 1999;285:901–906. [PubMed: 10436161]
34. Giaever G, Chu AM, Ni L, Connelly C, Riles L, Veronneau S, Dow S, Lucau-Danila A, Anderson K, Andre B, Arkin AP, Astromoff A, El-Bakkoury M, Bangham R, Benito R, Brachat S, Campanaro S, Curtiss M, Davis K, Deutschbauer A, Entian KD, Flaherty P, Foury F, Garfinkel DJ, Gerstein M, Gotte D, Guldener U, Hegemann JH, Hempel S, Herman Z, Jaramillo DF, Kelly DE, Kelly SL, Kotter P, LaBonte D, Lamb DC, Lan N, Liang H, Liao H, Liu L, Luo C, Lussier M, Mao R, Menard P, Ooi SL, Revuelta JL, Roberts CJ, Rose M, Ross-Macdonald P, Scherens B, Schimmack G, Shafer B, Shoemaker DD, Sookhai-Mahadeo S, Storms RK, Strathern JN, Valle G, Voet M, Volckaert G, Wang CY, Ward TR, Wilhelmy J, Winzeler EA, Yang Y, Yen G, Youngman E, Yu K, Bussey H, Boeke JD, Snyder M, Philippsen P, Davis RW, Johnston M. Functional profiling of the saccharomyces cerevisiae genome. Nature 2002;418:387–391. [PubMed: 12140549]
35. Paulovich AG, Armour CD, Hartwell LH. The saccharomyces cerevisiae RAD9, RAD17, RAD24 and MEC3 genes are required for tolerating irreparable, ultraviolet-induced DNA damage. Genetics 1998;150:75–93. [PubMed: 9725831]
36. Kadyk LC, Hartwell LH. Replication-dependent sister chromatid recombination in rad1 mutants of saccharomyces cerevisiae. Genetics 1993;133:469–487. [PubMed: 8454200]
37. Kadyk LC, Hartwell LH. Sister chromatids are preferred over homologs as substrates for recombinational repair in saccharomyces cerevisiae. Genetics 1992;132:387–402. [PubMed: 1427035]
38. Boone C, Bussey H, Andrews BJ. Exploring genetic interactions and networks with yeast. Nat Rev Genet 2007;8:437–449. [PubMed: 17510664]
39. Kai M, Furuya K, Paderi F, Carr AM, Wang TS. Rad3-dependent phosphorylation of the checkpoint clamp regulates repair-pathway choice. Nat Cell Biol 2007;9:691–697. [PubMed: 17515930]
40. Ostroff RM, Sclafani RA. Cell cycle regulation of induced mutagenesis in yeast. Mutat Res 1995;329:143–152. [PubMed: 7603496]
41. Lambert S, Watson A, Sheedy DM, Martin B, Carr AM. Gross chromosomal rearrangements and elevated recombination at an inducible site-specific replication fork barrier. Cell 2005;121:689–702. [PubMed: 15935756]
42. Tercero JA, Diffley JF. Regulation of DNA replication fork progression through damaged DNA by the Mec1/Rad53 checkpoint. Nature 2001;412:553–557. [PubMed: 11484057]
43. Al-Moghrabi NM, Al-Sharif IS, Aboussekhra A. The saccharomyces cerevisiae RAD9 cell cycle checkpoint gene is required for optimal repair of UV-induced pyrimidine dimers in both G(1) and G(2)/M phases of the cell cycle. Nucleic Acids Res 2001;29:2020–2025. [PubMed: 11353070]
44. Yu S, Teng Y, Lowndes NF, Waters R. RAD9, RAD24, RAD16 and RAD26 are required for the inducible nucleotide excision repair of UV-induced cyclobutane pyrimidine dimers from the transcribed and non-transcribed regions of the saccharomyces cerevisiae MFA2 gene. Mutat Res 2001;485:229–236. [PubMed: 11267834]
45. Al-Moghrabi NM, Al-Sharif IS, Aboussekhra A. The RAD9-dependent gene trans-activation is required for excision repair of active genes but not for repair of non-transcribed DNA. Mutat Res 2009;663:60–68. [PubMed: 19428371]
46. Reynolds AE, McCarroll RM, Newlon CS, Fangman WL. Time of replication of ARS elements along yeast chromosome III. Mol Cell Biol 1989;9:4488–4494. [PubMed: 2685553]
47. Rivin CJ, Fangman WL. Replication fork rate and origin activation during the S phase of saccharomyces cerevisiae. J Cell Biol 1980;85:108–115. [PubMed: 6767729]

48. Hanawalt PC, Spivak G. Transcription-coupled DNA repair: Two decades of progress and surprises. Nat Rev Mol Cell Biol 2008;9:958–970. [PubMed: 19023283]
49. Chang DJ, Cimprich KA. DNA damage tolerance: When it's OK to make mistakes. Nat Chem Biol 2009;5:82–90. [PubMed: 19148176]
50. Symington LS. Role of RAD52 epistasis group genes in homologous recombination and double-strand break repair. Microbiol Mol Biol Rev 2002;66:630–70. table of contents. [PubMed: 12456786]
51. Fabre F, Chan A, Heyer WD, Gangloff S. Alternate pathways involving Sgs1/Top3, Mus81/Mms4, and Srs2 prevent formation of toxic recombination intermediates from single-stranded gaps created by DNA replication. Proc Natl Acad Sci U S A 2002;99:16887–16892. [PubMed: 12475932]
52. Gangavarapu V, Prakash S, Prakash L. Requirement of RAD52 group genes for postreplication repair of UV-damaged DNA in Saccharomyces cerevisiae. Mol Cell Biol 2007;27:7758–7764. [PubMed: 17785441]
53. Branzei D, Vanoli F, Foiani M. SUMOylation regulates Rad18-mediated template switch. Nature 2008;456:915–920. [PubMed: 19092928]
54. Deng CX. BRCA1: Cell cycle checkpoint, genetic instability, DNA damage response and cancer evolution. Nucleic Acids Res 2006;34:1416–1426. [PubMed: 16522651]
55. Fong PC, Boss DS, Yap TA, Tutt A, Wu P, Mergui-Roelvink M, Mortimer P, Swaisland H, Lau A, O'Connor MJ, Ashworth A, Carmichael J, Kaye SB, Schellens JH, de Bono JS. Inhibition of poly (ADP-ribose) polymerase in tumors from BRCA mutation carriers. N Engl J Med 2009;361:123–134. [PubMed: 19553641]
56. Ball LG, Zhang K, Cobb JA, Boone C, Xiao W. The yeast shu complex couples error-free post-replication repair to homologous recombination. Mol Microbiol 2009;73:89–102. [PubMed: 19496932]
57. Ulrich HD, Jentsch S. Two RING finger proteins mediate cooperation between ubiquitin-conjugating enzymes in DNA repair. EMBO J 2000;19:3388–3397. [PubMed: 10880451]
58. Nelson JR, Lawrence CW, Hinkle DC. Deoxycytidyl transferase activity of yeast REV1 protein. Nature 1996;382:729–731. [PubMed: 8751446]
59. Duro E, Vaisica JA, Brown GW, Rouse J. Budding yeast Mms22 and Mms1 regulate homologous recombination induced by replisome blockage. DNA Repair (Amst) 2008;7:811–818. [PubMed: 18321796]
60. Bellaoui M, Chang M, Ou J, Xu H, Boone C, Brown GW. Elg1 forms an alternative RFC complex important for DNA replication and genome integrity. EMBO J 2003;22:4304–4313. [PubMed: 12912927]
61. Giannattasio M, Sabbioneda S, Minuzzo M, Plevani P, Muzi-Falconi M. Correlation between checkpoint activation and in vivo assembly of the yeast checkpoint complex Rad17-Mec3-Ddc1. J Biol Chem 2003;278:22303–22308. [PubMed: 12672803]
62. Xiao W, Derfler B, Chen J, Samson L. Primary sequence and biological functions of a saccharomyces cerevisiae O6-methylguanine/O4-methylthymine DNA repair methyltransferase gene. EMBO J 1991;10:2179–2186. [PubMed: 2065659]
63. Oh SD, Lao JP, Taylor AF, Smith GR, Hunter N. RecQ helicase, Sgs1, and XPF family endonuclease, Mus81-Mms4, resolve aberrant joint molecules during meiotic recombination. Mol Cell 2008;31:324–336. [PubMed: 18691965]
64. Morillon A, Karabetsou N, O'Sullivan J, Kent N, Proudfoot N, Mellor J. Isw1 chromatin remodeling ATPase coordinates transcription elongation and termination by RNA polymerase II. Cell 2003;115:425–435. [PubMed: 14622597]
65. Mathieu M, Modis Y, Zeelen JP, Engel CK, Abagyan RA, Ahlberg A, Rasmussen B, Lamzin VS, Kunau WH, Wierenga RK. The 1.8 A crystal structure of the dimeric peroxisomal 3-ketoacyl-CoA thiolase of saccharomyces cerevisiae: Implications for substrate binding and reaction mechanism. J Mol Biol 1997;273:714–728. [PubMed: 9402066]
66. Tong AH, Evangelista M, Parsons AB, Xu H, Bader GD, Page N, Robinson M, Raghibizadeh S, Hogue CW, Bussey H, Andrews B, Tyers M, Boone C. Systematic genetic analysis with ordered arrays of yeast deletion mutants. Science 2001;294:2364–2368. [PubMed: 11743205]
67. Brown SJ, Kellett PJ, Lippard SJ. Ixr1, a yeast protein that binds to platinated DNA and confers sensitivity to cisplatin. Science 1993;261:603–605. [PubMed: 8342024]

68. Mankouri HW, Ngo HP, Hickson ID. Esc2 and Sgs1 act in functionally distinct branches of the homologous recombination repair pathway in saccharomyces cerevisiae. Mol Biol Cell 2009;20:1683–1694. [PubMed: 19158388]

69. Rep M, Reiser V, Gartner U, Thevelein JM, Hohmann S, Ammerer G, Ruis H. Osmotic stress-induced gene expression in saccharomyces cerevisiae requires Msn1p and the novel nuclear factor Hot1p. Mol Cell Biol 1999;19:5474–5485. [PubMed: 10409737]

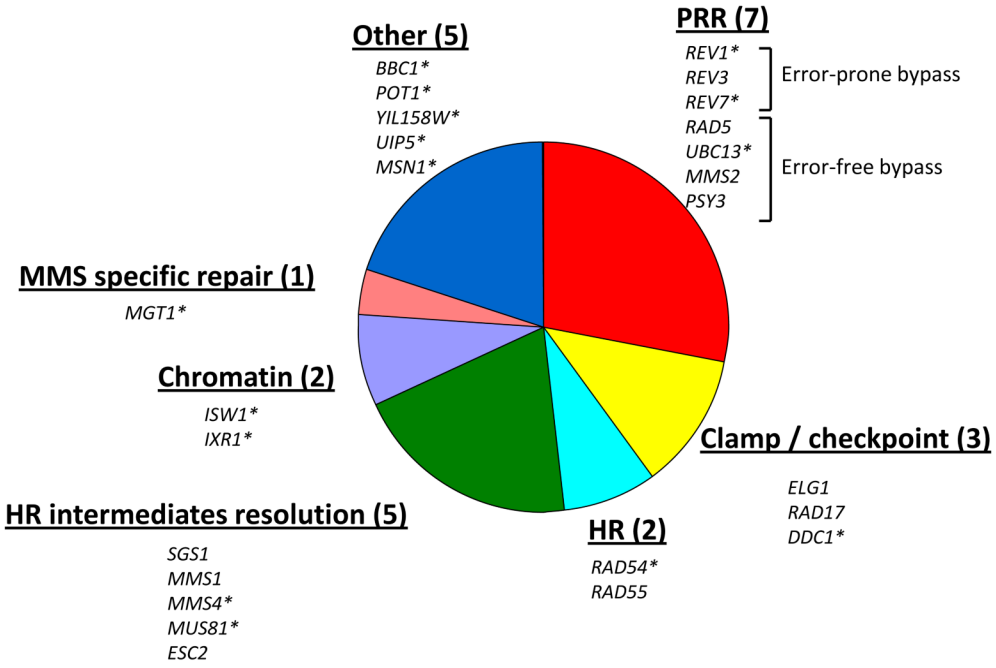

Figure 1.

Pie chart summarizing the results of the *rad9*Δ synthetic genetic screen in the presence of 0.01% methylmethane sulfonate (MMS). Genes were categorized according to their annotations in the Saccharomyces Genome Database (www.yeastgenome.org). The genes showing interactions with *RAD9* include genes functioning to accommodate DNA damage during replication and others that are previously unknown to be involved in the DNA damage response. Genes listed with asterisks represent interactions not previously identified. Fifteen novel *RAD9* genetic interactions were uncovered in this screen. Abbreviations are as follows: PRR, post-replication repair; HR, homologous recombination.

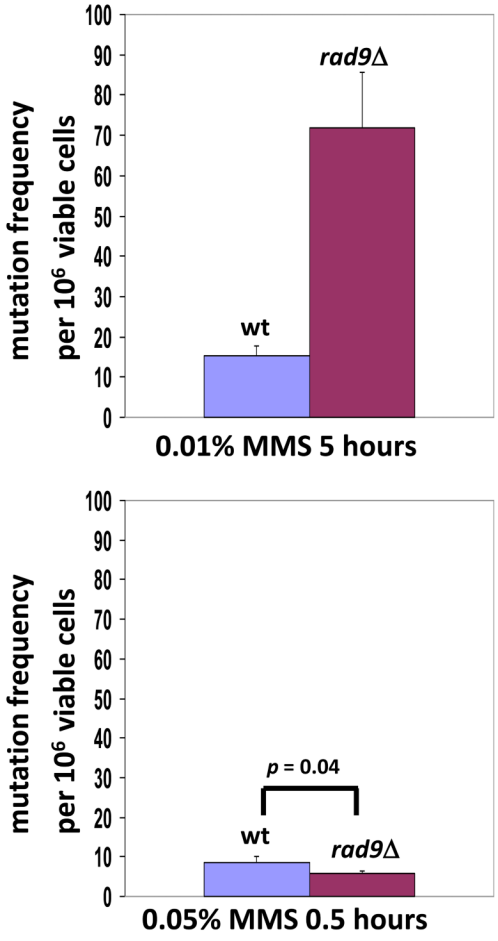

Figure 2A

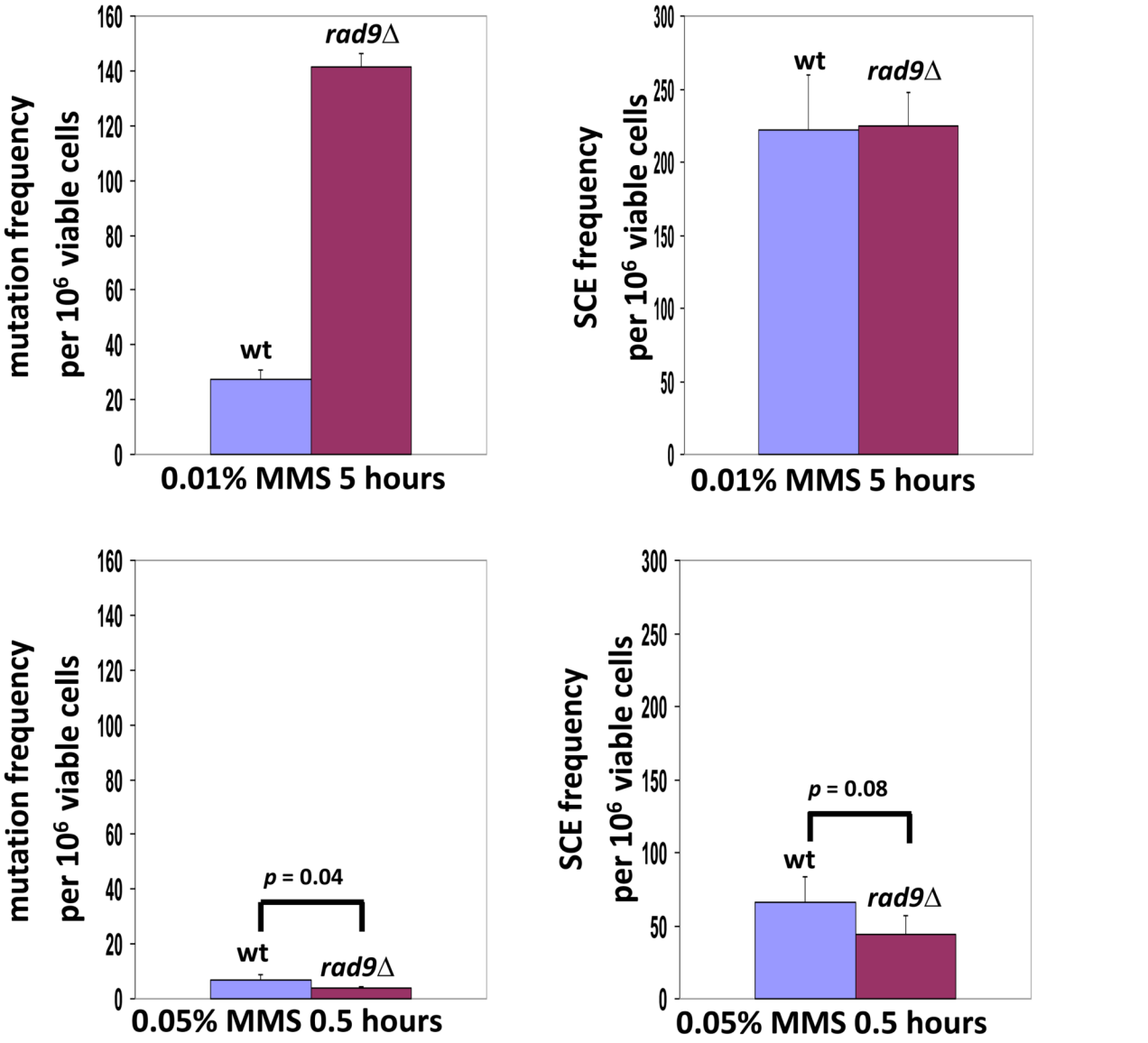

Figure 2B

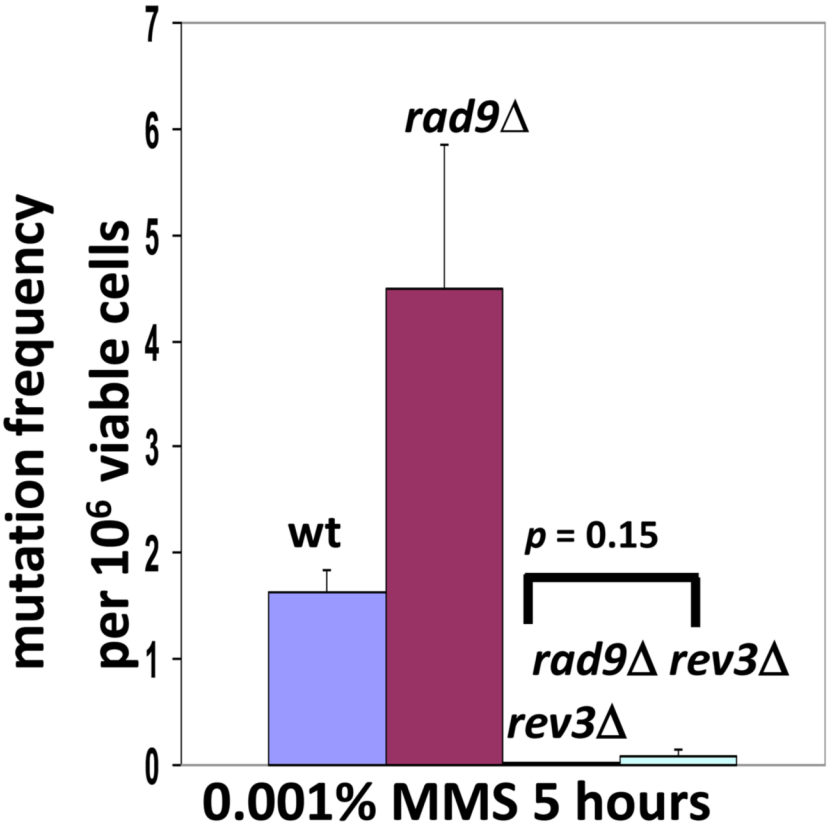

Figure 2C

Figure 2.

MMS dose-dependent hypermutation phenotype in the *rad9*Δ mutant. **A)** Log-phase wild type (BY4741) and *rad9*Δ (CB1021) cells (BY4741 background) were grown in the presence of 0.01% MMS for 5 hours and then harvested for determination of survival (62±5% and 4.8 ±0.5% for wild type and *rad9*Δ cells, respectively) and induction of mutation to Can^R (upper panel). In parallel, the survival and mutation rates were also determined for wild type and *rad9*Δ cells grown for a shorter time (0.5 hour) in higher-concentration (0.05%) of MMS (lower panel, the survival rate for wild type and *rad9*Δ were 98±3% and 73±4%, respectively). Each strain was tested in triplicate, and the error bars represent the standard deviations. **B)** Yeast cells from a different genetic background (A364a) were tested for mutation to Can^R as well as induction of SCE after MMS exposure (as above). The survival rate for wild type (yMP10381) and *rad9*Δ (yMP11030) were 79±6% and 3.1±0.2%, respectively in the 0.01%/5 hour MMS treatment; the survival rate for wild type and *rad9*Δ were 88±6% and 84±2%, respectively in the 0.05%/0.5 hour MMS treatment. Each strain was tested in triplicate, and the error bars represent standard deviations. **C)** The MMS-induced hypermutability of *rad9*Δ is *REV3*-dependent. Wild type (yMP10381), *rad9*Δ (yMP11030), *rev3*Δ (yMP10382), and *rad9*Δ *rev3*Δ (yDH51, yDH52, yDH53) cells were tested for survival and mutation to Can^R after treatment with a very low concentration of MMS (0.001%) for 5 hours (low concentration MMS was required due to the high sensitivity of the *rad9*Δ *rev3*Δ double mutant, Table 2). The survival rate for wild type, *rad9*Δ, *rev3*Δ and *rad9*Δ *rev3*Δ cells were 93±3%, 63±4%, 90 ±12% and 12±1%, respectively. Each strain was tested in triplicate, and the error bars represent standard deviations.

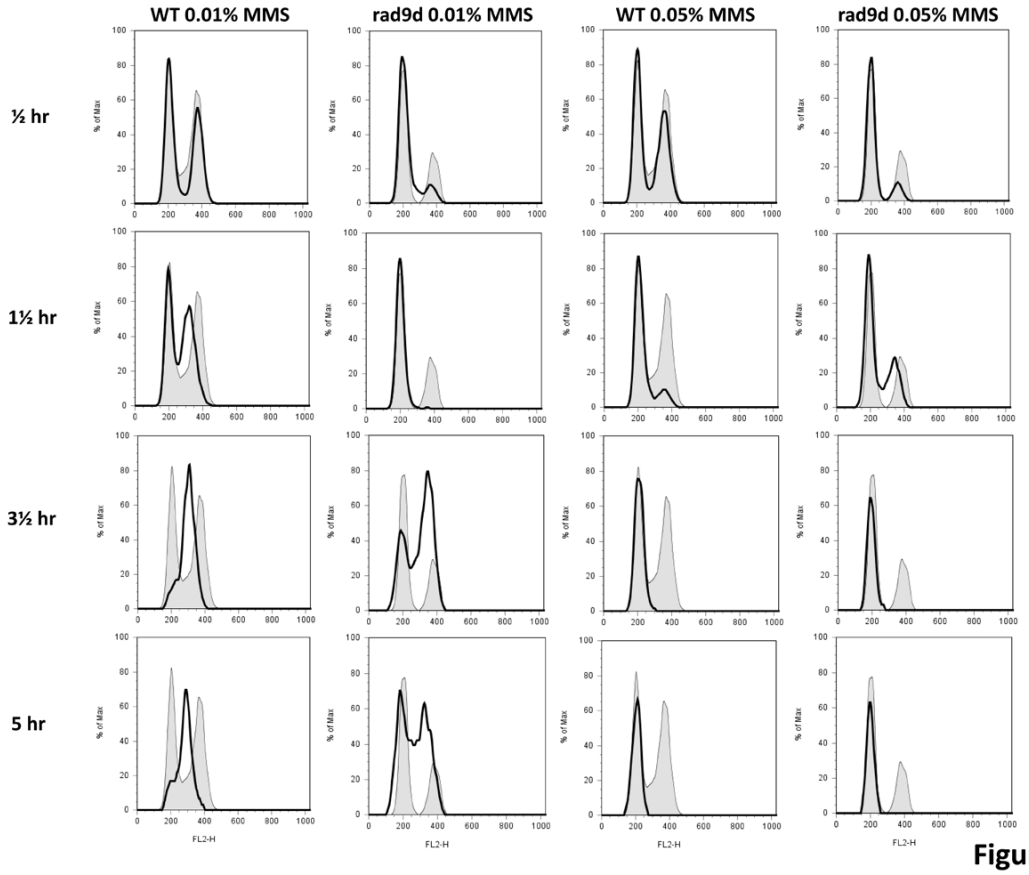

Figure 3A

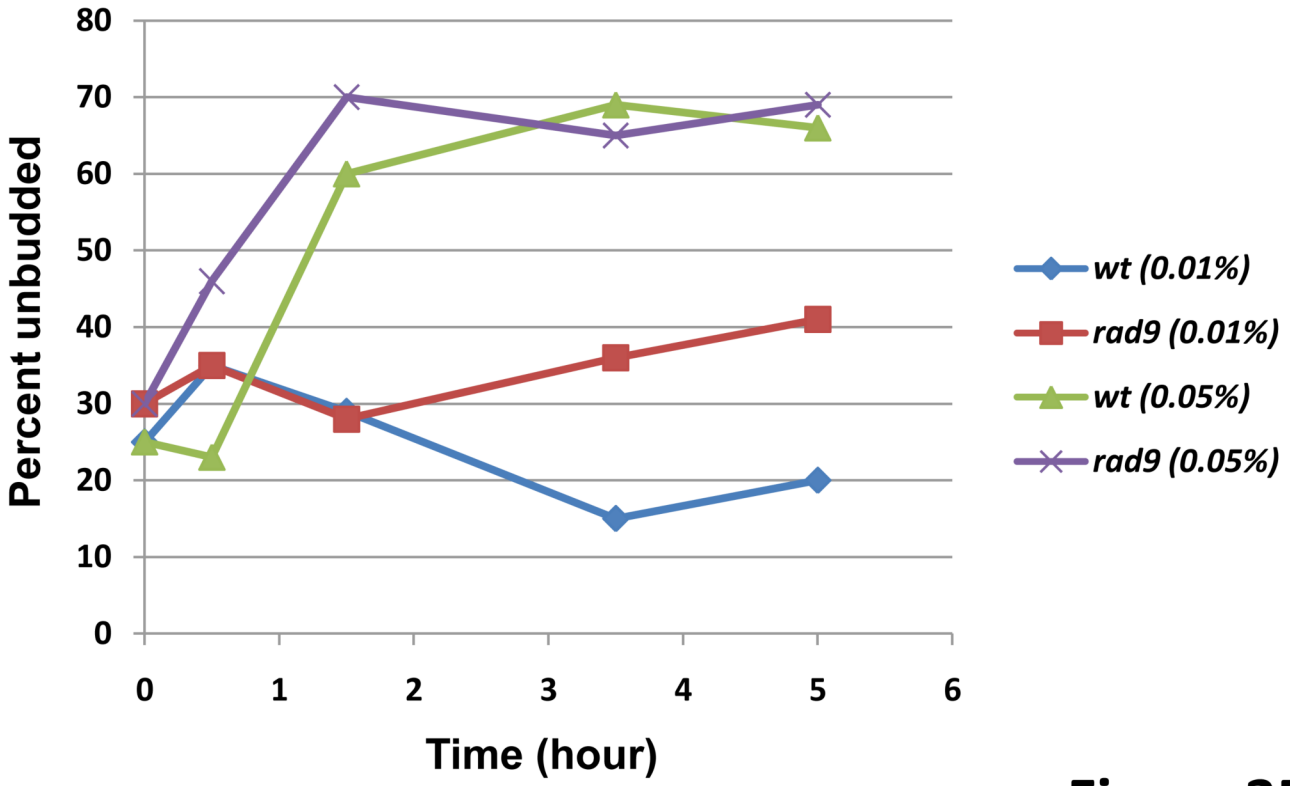

Figure 3B

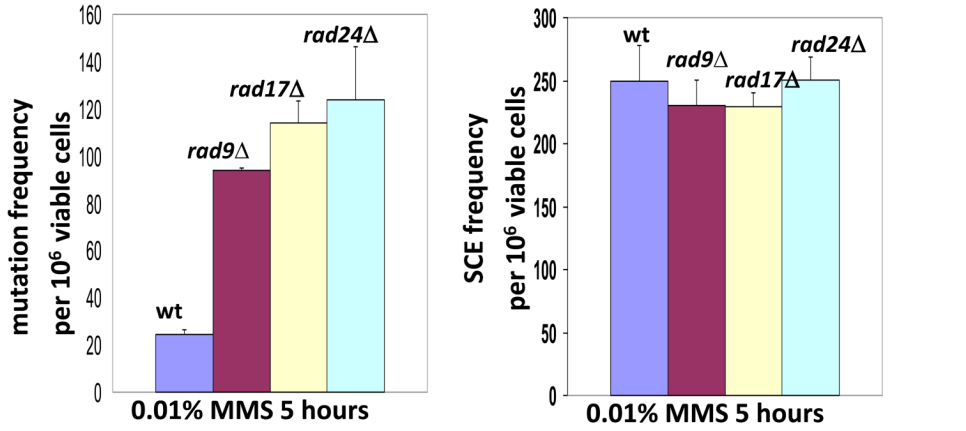

Figure 3C

Figure 3.

Relationship between the hypermutability phenotype and cell cycle distribution. **A)** Cell cycle redistribution following continuous exposure of asynchronous populations of wild type (yMP10381) or *rad9*Δ (yMP11030) cells to 0.01% and 0.05% MMS. At indicated times of exposure, samples were removed and analyzed by flow cytometry. Each panel contains two histograms. Shaded histograms represent the cell cycle distribution of the asynchronous culture, before addition of MMS. Overlaid histograms represent the cell cycle distribution at various times after addition of MMS. **B)** Percentage of unbudded cells at the indicated time during MMS exposure in liquid cultures for wild type and *rad9*Δ cells. **C)** Multiple intra-S phase checkpoint defective strains show hypermutability in 0.01% MMS. Wild type

(yMP10381), *rad9*Δ (yMP11030), *rad17*Δ (yMP11089), and *rad24*Δ (yMP11006) cells were tested for survival, mutation to Can^R and SCE after exposure to 0.01% MMS for 5 hours, as above. The survival rate for wild type, *rad9*Δ, *rad17*Δ, and *rad24*Δ cells were 66±8%, 3.5 ±0.3%, 4.1±0.2% and 1.7±0.2% respectively. Each strain was tested in triplicate, and the error bars represent standard deviations.

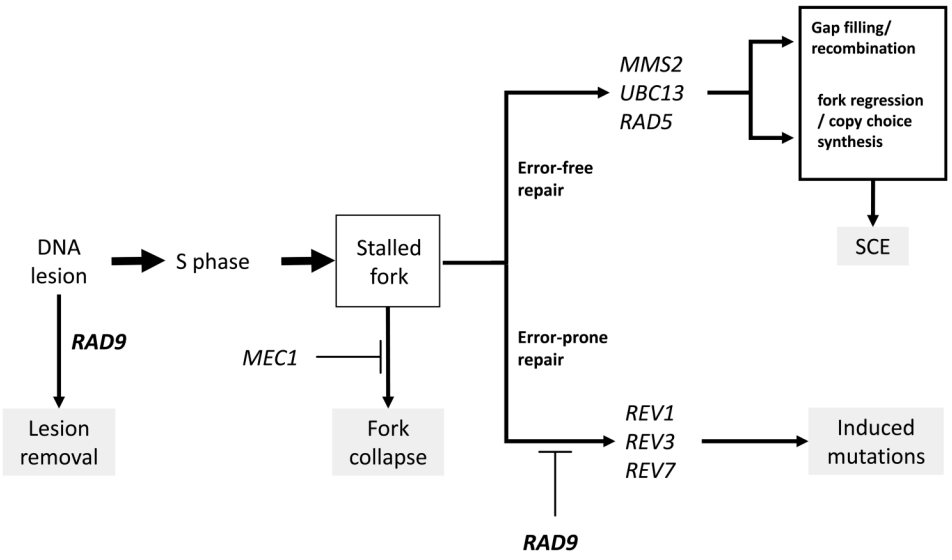

Figure 4.

One model proposing a role for *RAD9* in regulating how lesions are channeled at the replication fork. Under the model, in the presence of MMS, *RAD9* activity would strongly and *actively promote* use of non-mutagenic base excision repair (and/or alkylation reversal), while it would *actively suppress* mutagenic translesion synthesis. Hence, loss of *RAD9* function would reduce the efficacy of base excision repair, thereby increasing the reliance of cells on template switching and translesion synthesis for survival; this would explain the synergy observed between the *rad9*Δ and both the *mms2* and *rev3* mutants. Additionally, loss of *RAD9* function would result in derepression of translesion synthesis, resulting in the hypermutable phenotype observed in our experiments. Hence, under this model, *RAD9* stabilizes the genome by maximizing the cell's ability to employ non-mutagenic mechanisms (base excision repair and template switching) of repairing or tolerating lesions, while suppressing mutagenic translesion synthesis. As discussed in the text, a second alternative model is that *RAD9* acts to promote continuous DNA synthesis, potentially by limiting re-priming of stalled forks at MMS lesions. In this model, the observed hypermutability in MMS-treated *rad9*Δ cells may be due to an increased reliance on PRR to repair large ssDNA gaps resulting from discontinuous synthesis, which would explain the synergy between *rad9*Δ and both the *MMS2* and *REV3* branches of PRR.

TABLE 1

Saccharomyces cerevisiae Strains

Strain	Genotype	source
BY4741	*MAT***a** *his3Δ1 leu2Δ0 met15Δ0 ura3Δ0*	Open Biosystems
CB1021	*MAT***a** *ura3Δ0 leu2Δ0 his3Δ1 lys2Δ0 MET15 can1Δ::LEU2+-MFA1pr-HIS3 rad9::URA3*	This study
yAM1184-86	*MAT***a** *ura3Δ0 leu2Δ0 his3Δ1 lys2Δ0 MET15 can1Δ::LEU2+-MFA1pr-HIS3 sgs1::KAN^R*	This study
yAM1187-89	*MAT***a** *ura3Δ0 leu2Δ0 his3Δ1 lys2Δ0 MET15 can1Δ::LEU2+-MFA1pr-HIS3 sgs1::KAN^R rad9::URA3*	This study
yAM1202-4	*MAT***a** *ura3Δ0 leu2Δ0 his3Δ1 lys2Δ0 MET15 can1Δ::LEU2+-MFA1pr-HIS3 rev1::KAN^R*	This study
yAM1205-7	*MAT***a** *ura3Δ0 leu2Δ0 his3Δ1 lys2Δ0 MET15 can1Δ::LEU2+-MFA1pr-HIS3 rev1::KAN^R rad9::URA3*	This study
yAM1208-10	*MAT***a** *ura3Δ0 leu2Δ0 his3Δ1 lys2Δ0 MET15 can1Δ::LEU2+-MFA1pr-HIS3 rad17::KAN^R*	This study
yAM1211-13	*MAT***a** *ura3Δ0 leu2Δ0 his3Δ1 lys2Δ0 MET15 can1Δ::LEU2+-MFA1pr-HIS3 rad17::KAN^R rad9::URA3*	This study
yAM1214-16	*MAT***a** *ura3Δ0 leu2Δ0 his3Δ1 lys2Δ0 MET15 can1Δ::LEU2+-MFA1pr-HIS3 rad55::KAN^R*	This study
yAM1217-19	*MAT***a** *ura3Δ0 leu2Δ0 his3Δ1 lys2Δ0 MET15 can1Δ::LEU2+-MFA1pr-HIS3 rad55::KAN^R rad9::URA3*	This study
yAM1220-22	*MAT***a** *ura3Δ0 leu2Δ0 his3Δ1 lys2Δ0 MET15 can1Δ::LEU2+-MFA1pr-HIS3 isw1::KAN^R*	This study
yAM1223-25	*MAT***a** *ura3Δ0 leu2Δ0 his3Δ1 lys2Δ0 MET15 can1Δ::LEU2+-MFA1pr-HIS3 isw1::KAN^R rad9::URA3*	This study
yAM1226-28	*MAT***a** *ura3Δ0 leu2Δ0 his3Δ1 lys2Δ0 MET15 can1Δ::LEU2+-MFA1pr-HIS3 rev3::KAN^R*	This study
yAM1229-31	*MAT***a** *ura3Δ0 leu2Δ0 his3Δ1 lys2Δ0 MET15 can1Δ::LEU2+-MFA1pr-HIS3 rev3::KAN^R rad9::URA3*	This study
yAM1238-40	*MAT***a** *ura3Δ0 leu2Δ0 his3Δ1 lys2Δ0 MET15 can1Δ::LEU2+-MFA1pr-HIS3 ddc1::KAN^R*	This study
yAM1241-43	*MAT***a** *ura3Δ0 leu2Δ0 his3Δ1 lys2Δ0 MET15 can1Δ::LEU2+-MFA1pr-HIS3 ddc1::KAN^R rad9::URA3*	This study
yAM1244-46	*MAT***a** *ura3Δ0 leu2Δ0 his3Δ1 lys2Δ0 MET15 can1Δ::LEU2+-MFA1pr-HIS3 ubc13::KAN^R*	This study
yAM1247-49	*MAT***a** *ura3Δ0 leu2Δ0 his3Δ1 lys2Δ0 MET15 can1Δ::LEU2+-MFA1pr-HIS3 ubc13::KAN^R rad9::URA3*	This study
yAM1250-52	*MAT***a** *ura3Δ0 leu2Δ0 his3Δ1 lys2Δ0 MET15 can1Δ::LEU2+-MFA1pr-HIS3 esc2::KAN^R*	This study
yAM1253-55	*MAT***a** *ura3Δ0 leu2Δ0 his3Δ1 lys2Δ0 MET15 can1Δ::LEU2+-MFA1pr-HIS3 esc2::KAN^R rad9::URA3*	This study
yAM1280-82	*MAT***a** *ura3Δ0 leu2Δ0 his3Δ1 lys2Δ0 MET15 can1Δ::LEU2+-MFA1pr-HIS3 mus81::KAN^R*	This study
yAM1283-85	*MAT***a** *ura3Δ0 leu2Δ0 his3Δ1 lys2Δ0 MET15 can1Δ::LEU2+-MFA1pr-HIS3 mus81::KAN^R rad9::URA3*	This study
yAM1286-88	*MAT***a** *ura3Δ0 leu2Δ0 his3Δ1 lys2Δ0 MET15 can1Δ::LEU2+-MFA1pr-HIS3 rad5::KAN^R*	This study
yAM1289-91	*MAT***a** *ura3Δ0 leu2Δ0 his3Δ1 lys2Δ0 MET15 can1Δ::LEU2+-MFA1pr-HIS3 rad5::KAN^R rad9::URA3*	This study
yAM1292-94	*MAT***a** *ura3Δ0 leu2Δ0 his3Δ1 lys2Δ0 MET15 can1Δ::LEU2+-MFA1pr-HIS3 msn1::KAN^R*	This study
yAM1295-97	*MAT***a** *ura3Δ0 leu2Δ0 his3Δ1 lys2Δ0 MET15 can1Δ::LEU2+-MFA1pr-HIS3 msn1::KAN^R rad9::URA3*	This study
yAM1304-6	*MAT***a** *ura3Δ0 leu2Δ0 his3Δ1 lys2Δ0 MET15 can1Δ::LEU2+-MFA1pr-HIS3 uip5::KAN^R*	This study
yAM1307-9	*MAT***a** *ura3Δ0 leu2Δ0 his3Δ1 lys2Δ0 MET15 can1Δ::LEU2+-MFA1pr-HIS3 uip5::KAN^R rad9::URA3*	This study
yAM1328-30	*MAT***a** *ura3Δ0 leu2Δ0 his3Δ1 lys2Δ0 MET15 can1Δ::LEU2+-MFA1pr-HIS3 mgt1::KAN^R*	This study
yAM1331-33	*MAT***a** *ura3Δ0 leu2Δ0 his3Δ1 lys2Δ0 MET15 can1Δ::LEU2+-MFA1pr-HIS3 mgt1::KAN^R rad9::URA3*	This study
yAM1340-42	*MAT***a** *ura3Δ0 leu2Δ0 his3Δ1 lys2Δ0 MET15 can1Δ::LEU2+-MFA1pr-HIS3 bbc1::KAN^R*	This study
yAM1343-45	*MAT***a** *ura3Δ0 leu2Δ0 his3Δ1 lys2Δ0 MET15 can1Δ::LEU2+-MFA1pr-HIS3 bbc1::KAN^R rad9::URA3*	This study
yAM1370-72	*MAT***a** *ura3Δ0 leu2Δ0 his3Δ1 lys2Δ0 MET15 can1Δ::LEU2+-MFA1pr-HIS3 mms2::KAN^R*	This study
yAM1373-75	*MAT***a** *ura3Δ0 leu2Δ0 his3Δ1 lys2Δ0 MET15 can1Δ::LEU2+-MFA1pr-HIS3 mms2::KAN^R rad9::URA3*	This study
yAM1388-90	*MAT***a** *ura3Δ0 leu2Δ0 his3Δ1 lys2Δ0 MET15 can1Δ::LEU2+-MFA1pr-HIS3 mms1::KAN^R*	This study
yAM1391-93	*MAT***a** *ura3Δ0 leu2Δ0 his3Δ1 lys2Δ0 MET15 can1Δ::LEU2+-MFA1pr-HIS3 mms1::KAN^R rad9::URA3*	This study
yAM1394-96	*MAT***a** *ura3Δ0 leu2Δ0 his3Δ1 lys2Δ0 MET15 can1Δ::LEU2+-MFA1pr-HIS3 pot1::KAN^R*	This study
yAM1397-99	*MAT***a** *ura3Δ0 leu2Δ0 his3Δ1 lys2Δ0 MET15 can1Δ::LEU2+-MFA1pr-HIS3 pot1::KAN^R rad9::URA3*	This study

Strain	Genotype	source
yAM1418-20	*MAT***a** *ura3Δ0 leu2Δ0 his3Δ1 lys2Δ0 MET15 can1Δ::LEU2+-MFA1pr-HIS3 rev7::KAN^R*	This study
yAM1421-23	*MAT***a** *ura3Δ0 leu2Δ0 his3Δ1 lys2Δ0 MET15 can1Δ::LEU2+-MFA1pr-HIS3 rev7::KAN^R rad9::URA3*	This study
yAM1448-50	*MAT***a** *ura3Δ0 leu2Δ0 his3Δ1 lys2Δ0 MET15 can1Δ::LEU2+-MFA1pr-HIS3 mms4::KAN^R*	This study
yAM1451-53	*MAT***a** *ura3Δ0 leu2Δ0 his3Δ1 lys2Δ0 MET15 can1Δ::LEU2+-MFA1pr-HIS3 mms4::KAN^R rad9::URA3*	This study
yAM1454-56	*MAT***a** *ura3Δ0 leu2Δ0 his3Δ1 lys2Δ0 MET15 can1Δ::LEU2+-MFA1pr-HIS3 rad54::KAN^R*	This study
yAM1457-79	*MAT***a** *ura3Δ0 leu2Δ0 his3Δ1 lys2Δ0 MET15 can1Δ::LEU2+-MFA1pr-HIS3 rad54::KAN^R rad9::URA3*	This study
yAM1472-74	*MAT***a** *ura3Δ0 leu2Δ0 his3Δ1 lys2Δ0 MET15 can1Δ::LEU2+-MFA1pr-HIS3 yil158w::KAN^R*	This study
yAM1475-77	*MAT***a** *ura3Δ0 leu2Δ0 his3Δ1 lys2Δ0 MET15 can1Δ::LEU2+-MFA1pr-HIS3 yil158w::KAN^R rad9::URA3*	This study
yAM1490-92	*MAT***a** *ura3Δ0 leu2Δ0 his3Δ1 lys2Δ0 MET15 can1Δ::LEU2+-MFA1pr-HIS3 psy3::KAN^R*	This study
yAM1493-95	*MAT***a** *ura3Δ0 leu2Δ0 his3Δ1 lys2Δ0 MET15 can1Δ::LEU2+-MFA1pr-HIS3 psy3::KAN^R rad9::URA3*	This study
yAM1655-57	*MAT***a** *ura3Δ0 leu2Δ0 his3Δ1 lys2Δ0 MET15 can1Δ::LEU2+-MFA1pr-HIS3 ixr1::KAN^R*	This study
yAM1658-60	*MAT***a** *ura3Δ0 leu2Δ0 his3Δ1 lys2Δ0 MET15 can1Δ::LEU2+-MFA1pr-HIS3 ixr1::KAN^R rad9::URA3*	This study
yMP10381	*MAT***a** *ade2 ade3-130 leu2 trp1 ura3 cyh2 SCR::URA3*	Paulovich Lab
yMP10382	*MAT***a** *ade2 ade3-130 leu2 trp1 ura3 cyh2 rev3Δ::LEU2 SCR::URA3*	Paulovich Lab
yMP11006	*MAT***a** *ade2 ade3-130 leu2 trp1 ura3 cyh2 rad24Δ::TRP1 SCR::URA3*	Paulovich Lab
yMP11030	*MAT***a** *ade2 ade3-130 leu2 trp1 ura3 cyh2 SCR::URA3 rad9Δ::LEU2*	Paulovich Lab
yMP11089	*MAT***a** *ade2 ade3-130 leu2 trp1 ura3 cyh2 rad17Δ::LEU2 SCR::URA3*	Paulovich Lab
yMP11450	*MAT***a** *ade2 ade3-130 leu2 trp1 ura3 cyh2 SCR::URA3 rad52Δ::LEU2*	Paulovich Lab
yDH27-29	*MAT***a** *ade2 ade3-130 leu2 trp1 ura3 cyh2 bbc1Δ::KAN^r SCR::URA3*	This study
yDH30-32	*MAT***a** *ade2 ade3-130 leu2 trp1 ura3 cyh2 rad9Δ::LEU2 bbc1Δ::KAN^r SCR::URA3*	This study
yDH33-35	*MAT***a** *ade2 ade3-130 leu2 trp1 ura3 cyh2 isw1Δ::KAN^r SCR::URA3*	This study
yDH36-38	*MAT***a** *ade2 ade3-130 leu2 trp1 ura3 cyh2 rad9Δ::LEU2 isw1Δ::KAN^r SCR::URA3*	This study
yDH39-41	*MAT***a** *ade2 ade3-130 leu2 trp1 ura3 cyh2 yil158wΔ::KAN^r SCR::URA3*	This study
yDH42-44	*MAT***a** *ade2 ade3-130 leu2 trp1 ura3 cyh2 rad9Δ::LEU2 yil158wΔ::KAN^r SCR::URA3*	This study
yDH45-47	*MAT***a** *ade2 ade3-130 leu2 trp1 ura3 cyh2 pot1Δ::KAN^r SCR::URA3*	This study
yDH48-50	*MAT***a** *ade2 ade3-130 leu2 trp1 ura3 cyh2 rad9Δ::LEU2 pot1Δ::KAN^r SCR::URA3*	This study
yDH51-53	*MAT***a** *ade2 ade3-130 leu2 trp1 ura3 cyh2 rev3Δ::LEU2 rad9Δ::KAN^r SCR::URA3*	This study
yDH54-56	*MAT***a** *ade2 ade3-130 leu2 trp1 ura3 cyh2 rev3Δ::LEU2 bbc1Δ::KAN^r SCR::URA3*	This study
yDH57-59	*MAT***a** *ade2 ade3-130 leu2 trp1 ura3 cyh2 rev3Δ::LEU2 isw1Δ::KAN^r SCR::URA3*	This study
yDH60-62	*MAT***a** *ade2 ade3-130 leu2 trp1 ura3 cyh2 rev3Δ::LEU2 yil158wΔ::KAN^r SCR::URA3*	This study
yDH63-65	*MAT***a** *ade2 ade3-130 leu2 trp1 ura3 cyh2 rev3Δ::LEU2 pot1Δ::KAN^r SCR::URA3*	This study
yDH66-68	*MAT***a** *ade2 ade3-130 leu2 trp1 ura3 cyh2 rad52Δ::LEU2 bbc1Δ::KAN^r SCR::URA3*	This study
yDH69-71	*MAT***a** *ade2 ade3-130 leu2 trp1 ura3 cyh2 rad52Δ::LEU2 isw1Δ::KAN^r SCR::URA3*	This study
yDH72-74	*MAT***a** *ade2 ade3-130 leu2 trp1 ura3 cyh2 rad52Δ::LEU2 yil158wΔ::KAN^r SCR::URA3*	This study
yDH75-77	*MAT***a** *ade2 ade3-130 leu2 trp1 ura3 cyh2 rad52Δ::LEU2 pot1Δ::KAN^r SCR::URA3*	This study

CB1021 is congenic with BY4741 (S288C). The yAM strains are isogenic with CB1021. The remaining strains are all congenic with yMP10381 (A364a).

TABLE 2

RAD9-interacting genes

Gene	Class[e]	Viability for single (%) (*xxx*Δ)[a]	Viability for double (%) (*xxx*Δ *rad9*Δ)[a]	Ratio[b]	*p* value[c]
RAD5	**Error-free bypass**	0.016±0.01	0[d]	∞[d]	ND[d]
UBC13	**Error-free bypass**	12±2	0.023±0.02	357.7	0.0015
REV7	**Error-prone bypass**	31±3	0.037±0.04	223.1	0.0015
MMS2	**Error-free bypass**	15±1	0.078±0.012	172.8	0.0011
REV1	**Error-prone bypass**	60±21	0.12±0.10	64.7	0.0016
RAD54	**HR**	12±6	0.17±0.11	47.4	0.0016
REV3	**Error-prone bypass**	76±15	0.20±0.12	40.8	0.0016
MMS1	**HR intermediate resolution**	54±8	0.25±0.05	33.0	0.0016
ELG1	**Clamp loader**	28±1	0.37±0.22	22.4	0.0018
DDC1	**9-1-1 complex**	12±2	0.41±0.10	20.4	0.0017
MGT1	**Methyltransferase**	39±6	0.42±0.16	19.9	0.0018
MUS81	**HR intermediate resolution**	2.7±0.4	0.14±0.05	18.9	0.0040
MMS4	**HR intermediate resolution**	3.6±0.2	0.20±0.09	17.8	0.0011
ISW1	Chromatin	41±12	0.52±0.17	16.1	0.0018
POT1	Fatty acid oxidation	34±14	0.54±0.41	15.4	0.0022
RAD17	**9-1-1 complex**	6±0.7	0.43±0.09	14.2	0.0028
SGS1	**HR intermediate resolution**	28±5	0.67±0.23	12.5	0.0020
RAD55	**HR**	18±8	0.70±0.33	12.0	0.0021
BBC1	Actin patch	84±24	0.73±0.65	11.4	0.0030
IXR1	Chromatin	29±10	0.99±0.29	8.4	0.0022
YIL158W	unknown	60±11	1.3±0.8	6.3	0.0047
ESC2	**HR intermediate resolution**	18±5	1.3±0.9	6.1	0.0050
UIP5	unkown	29±4	1.4±0.3	5.8	0.0027
PSY3	**Error-free bypass**	30±11	1.5±0.5	5.5	0.0035
MSN1	Transcription	24±6	1.6±0.8	5.0	0.0048

[a] Cells were exposed to 0.01% MMS in liquid rich medium for 5 hours. Wild type is BY4741 (S288C). Error represents the standard deviation calculated for three independent biological experiments performed on three subsequent days on three independent segregants for each double mutant. After MMS treatment, the survival rate for wild type and *rad9*Δ strains are 76±13% and 8.3±0.8%.

[b] Ratio is calculated as the viability of the most sensitive single mutant (i.e. either *rad9*Δ or *xxx*Δ) versus the viability of the *rad9*Δ *xxx*Δ double mutant.

[c] The *p*-values for the reliability of the difference of survival rates between the single and double mutants were calculated using t-tests.

[d] There were no viable colonies for the *rad*5Δ *rad*9Δ double mutant after 5 hour exposure to 0.01% MMS; 2×10^4 cells were plated; hence, viability was ≤ 0.005%. (p-value can not be accurately calculated.)

[e] Gene functions are classified according to annotations in Saccharomyces Genome Database (www.yeastgenome.org) and the literature referenced in the database (see Supplemental table S1). *PSY3* was very recently assigned to the error-free bypass branch of PRR pathway by Ball et al[56].

DNA Repair (Amst). Author manuscript; available in PMC 2011 July 1.